

Amthor, Arvid; Hausotte, Tino; Ament, Christoph; Li, Pu;
Jäger, Gerd :

Friction identification and compensation on nanometer scale

Publikation entstand im Rahmen der Veranstaltung:
17th IFAC World Congress, July 6 - 11, 2008, Seoul, Korea

FRICITION IDENTIFICATION AND COMPENSATION ON NANOMETER SCALE

A. Amthor*, T. Hausotte**,
Ch. Ament*, P. Li*, G. Jaeger**

**Institute of Automation and Systems Engineering, Technische Universität Ilmenau,
Germany (e-mail: arvid.amthor@tu-ilmenau.de).*

***Institute of Process Measurement and Sensor Technology, Technische Universität Ilmenau,
Germany (e-mail: tino.hausotte@tu-ilmenau.de)*

Abstract: This work concerns the modelling and experimental verification of the highly nonlinear friction behavior in positioning on the nanometer scale. The main goal of this work is to adjust and identify a simple dynamic friction model which allows a model-based estimation of the friction force in combination with the system inertia against displacement. Experiments in the pre-sliding and sliding friction regimes are conducted on an experimental setup. A hybrid two-stage parameter estimation algorithm is used to fit the model parameters based on the experimental data. Finally, the identified friction model is utilized as a model-based feedforward controller combined with a classical feedback controller to compensate the nonlinear friction force and reduce tracking errors.

1. INTRODUCTION

In the field of micro- and nanotechnologies positioning with an extremely high resolution (below 1 nm) it is necessary to measure or manipulate surfaces on the atomic level. For this task, high resolution positioning tables are used nowadays. The position of these tables is always controlled by a feedback controller to avoid position errors caused by disturbances such as thermal expansion of the mechanical components, sound waves, ground motion and so on. If a positioning table with a big operating range is considered, one of the main disturbances, in particular during dynamic motion, is the friction introduced by the commonly used ball bearing guides. Friction is a highly nonlinear phenomenon which is present in nearly all mechanical systems. It is induced by interactions between the two rubbing surfaces and depends on several parameters such as surface topography, surface materials, the lubricant used etc. The friction force can be differentiated into two regimes: the pre-sliding (micro-slip) and the sliding (gross sliding) regime. In the first case adhesive forces holding the rubbing surfaces together are causing the friction force to behave like a nonlinear spring. In the sliding regime contacts between the asperities are broken and the friction force depends only on the shearing resistance of the surface asperities. The transition between the two regimes mentioned is continuous and depends on many effects such as direction of movement, rate of the applied force and others. With a linearly controlled motion these nonlinear system characteristics lead to tracking errors, limit cycles, stick-slip motion and so on (Armstrong-Héouvy, *et al.* 1994). Due to this dominant nonlinear impact, modelling friction is essential to achieve high-precision dynamic positioning. This is quite a challenging task since accurate friction modelling based on physical principles and material/surface properties is not possible to date. Hence “Greybox” and “Blackbox” models in combination with efficient identification methods based upon experimentally

observed data are often used to address this problem (Al-Bender *et al.* 2007).

In this work, we consider a highly nonlinear system in the pre-sliding and sliding friction regimes. A two-stage method is used to identify the parameters of a model of an experimental setup. After discussing some known approaches to express the friction dynamics mathematically, the experimental setup is explained. Then, the friction modelling process is presented. Next, a model-based control scheme is proposed with a modified model. It is shown by experimental results that this modification is able to significantly improve the performance of the control system used.

2. PHYSICALLY MOTIVATED FRICTION MODELS

This section gives a short review of the fundamental dynamic friction models, e.g. the Dahl model, the LuGre model and the generalised Maxwell-Slip model in combination with the related DNLRX identification method.

2.1 The Dahl Model

Dahl was the first to develop a dynamic friction model (Dahl 1968). Through many experiments on servo systems with ball bearings, he found that bearing friction demonstrates the same behaviour as solid friction. Dahl described the friction dynamics using a modified stress-strain curve of classical solid mechanics:

$$\frac{f}{dt} = \sigma \left(1 - \frac{f}{F_c} \cdot \operatorname{sgn} \left(\frac{dx}{dt} \right) \right)^\alpha \cdot \frac{dx}{dt} \quad (1)$$

Where f represents the friction force, σ the stiffness coefficient, α a shape parameter, F_c the Coulomb friction force and x the position. This is a generalization of the ordinary Coulomb friction model and captures some pre-

sliding and hysteresis-related phenomena. However, this model can not reflect the Stribeck and stiction effects.

2.2 The LuGre Friction Model

In order to overcome these drawbacks, Haessig and Friedland proposed to describe rough surfaces with a conglomerate of elastic bristles (Haessig and Friedland 1991). The idea of this is shown in figure 1.

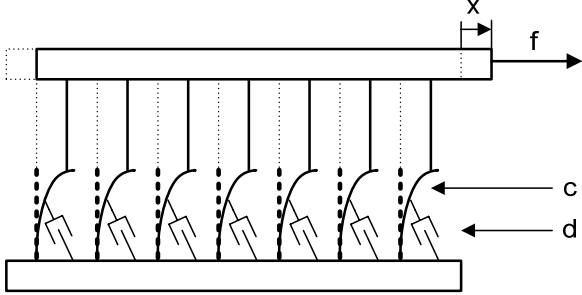


Fig. 1. Schematic illustration of the bristle model

If the two interacting surfaces are moving to each other the bristles deflect and begin to slide when the displacement is sufficient. The deflection of the bristles is expressed with the state variable z . In order to reduce the model dimension every bristle has the same state z and the bristles of one side are assumed as stiff.

The most commonly used representative of this group is the Lund-Grenoble (LuGre) model (De Wit *et al.* 1995). It describes the friction dynamics using Equ. (2) to (4):

$$f = \sigma_0 \cdot z + \sigma_1 \cdot \frac{dz}{dt} + \sigma_2 \cdot \frac{dx}{dt} \quad (2)$$

$$\frac{dz}{dt} = \frac{dx}{dt} - \frac{\left| \frac{dx}{dt} \right|}{g\left(\frac{dx}{dt}\right)} \cdot z \quad (3)$$

$$g\left(\frac{dx}{dt}\right) = \frac{1}{\sigma_0} \cdot \left[F_c + (F_s - F_c) e^{-\left(\frac{dx}{dt}\right)^\beta} \right] \quad (4)$$

In Equ. (2), the friction force is calculated using a spring and damper force caused by the bristles and a micro-viscous velocity-dependent part. The bristle state z is calculated by Equ. (3), where velocity is used as the input signal. $g(v)$ in Equ. (4) describes the Stribeck curve by utilising an e-function. F_c stands for the Coulomb friction force, F_s for the breakaway force, v_s for the Stribeck velocity and σ_0 for the micro-elastic bristle stiffness. This model is quite simple and able to capture sliding and pre-sliding behaviour in just one state equation. These properties make the LuGre model very popular in practical control engineering. Nevertheless, the LuGre model fails to describe some pre-sliding phenomena satisfactory e.g. the non-drifting property. Dupont, *et al.* (2002) extended the LuGre model to the so-called elasto-plastic friction model. They changed the determination of the

state variable z to enable the model to meet the non-drifting property. However, the elasto-plastic friction model cannot capture all pre-sliding phenomena.

2.3 The Generalized Maxwell-Slip Friction Model

Based on the integrated friction model, called the Leuven model (Lampaert *et al.* 2002, Lampaert *et al.* 2005) Lampaert described the friction dynamics with a totally different approach shown in figure 2.

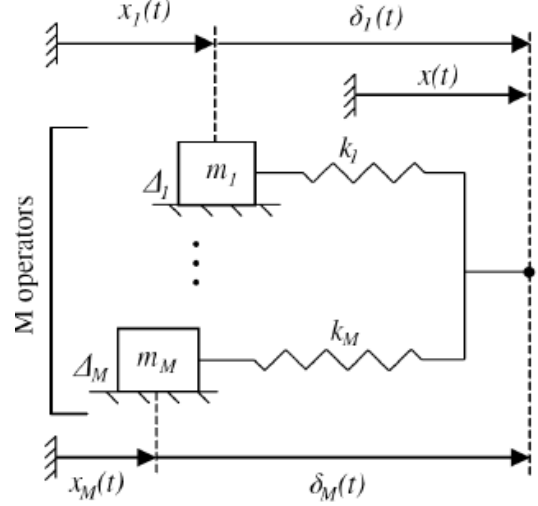


Fig. 2. Visualization of the Maxwell-slip approach

The idea is based on the assumption of modelling friction with M elasto-plastic elements in parallel, all having displacement as a common input. Each of these elements generates an output force F_i . A single element is characterised by a certain stiffness k_i , a slipping force limit Δ_i and a state variable δ_i . Since it is assumed that the elements have no mass, there exists a static relationship between the force F_i and the deflection of the springs δ_i . With this approach it is possible to capture the hysteresis with non-local memory (Lampaert *et al.* 2004).

$$f = \sum_{i=1}^N \left(k_i \cdot \delta_i + \sigma_i \cdot \frac{d\delta_i}{dt} \right) + fcn\left(\frac{dx}{dt}\right) \quad (5)$$

$$\frac{d\delta_i}{dt} = \frac{dx}{dt} \quad (6)$$

$$\frac{d\delta_i}{dt} = \text{sgn}\left(\frac{dx}{dt}\right) C_i \left(1 - \frac{\delta_i}{g_i\left(\frac{dx}{dt}\right)} \right) \quad (7)$$

Equ. (5) to (7) represent the generalised Maxwell-Slip (GMS) model structure. $fcn(v)$ is the so-called velocity-strengthening, or “viscous”, component of the friction force that is usually set to be proportional to v . $g_i(v)$ is the Stribeck curve (see Equ. (4)) and C_i a viscoelastic coefficient. To simplify the model, $g_i(v)$ and C_i are considered as common for all elements. A scaling parameter γ_i is introduced to extend the degrees of freedom, so that $g_i(v) = \gamma_i \cdot g(v)$ and $C_i = \gamma_i \cdot C$. The

drawback of the GMS model is the fact, that in many cases the immeasurable velocity is required as an input. Another shortcoming of the GMS model is the high experimental effort, which is needed to identify the model parameters.

2.4 The Dynamic NonLinear Regression with direct application of eXcitation (DNLRX) Identification Method

(Rizos *et al.* 2002a) considered a simple mechanical system with friction. It consists of a mass m , a linear spring with the spring constant c and a damper with the damping coefficient d (see figure 3). The system is stimulated by a force u and the (immeasurable) friction force f resists the excited motion.

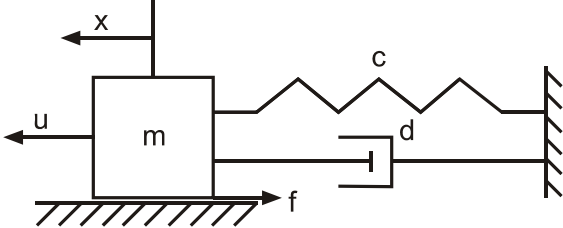


Fig. 3. Simple mechanical system with friction

The system can be described as follows:

$$m \cdot a(t) + d \cdot \frac{dx(t)}{dt} + c \cdot x(t) = u(t) - f(t) \quad (8)$$

$a(t)$ is the acceleration and $x(t)$ the displacement. The acceleration and velocity needed can be approximated with moving average representations of orders n_v and n_a and the coefficients p_i and q_i , respectively:

$$v(k) \approx \sum_{j=0}^{n_v} p_i \cdot x(k-j) \quad \text{with } t = k \cdot T \quad (9)$$

$$a(k) \approx \sum_{j=0}^{n_a} q_i \cdot x(k-j) \quad \text{with } t = k \cdot T \quad (10)$$

with T is the used sample time. To determine the spring deformation of each Maxwell-slip element, a modified version of the GMS Equ. (6) and (7) in discrete time is utilised:

$$\delta_i(k+1) = \text{sgn} [x(k+1) - x(k) + \delta_i(k)] \cdot \min \{ |x(k+1) - x(k) + \delta_i(k)|, \Delta_i \} \quad (11)$$

In addition to the spring deformations in this modified GMS model, the friction force also depends on the displacement history and can be expressed in discrete time as:

$$f(k) = \sum_{j=0}^{n_x} r_j \cdot x(k-j) + \sum_{j=0}^{n_\delta} \Theta_j^T \cdot \delta(k-j) \quad (12)$$

Equ. (12) suggests that the friction force is calculated by having the displacement driven through a finite impulse response (FIR) filter of order n_x (with coefficients r_j for $j = 0, \dots, n_x$) and the spring deformation vector $\delta(k) = [\delta_1(k) \dots \delta_M(k)]^T$ driven through a M -dimensional FIR filter of order n_δ (with vector coefficients Θ_j for $j = 0, \dots, n_\delta$).

Equs. (9), (10) and (12) represent approximations of acceleration, velocity and friction force based on the displacement history. Placing these expressions into Equ. (8) leads to a time-discrete system model:

$$m \cdot \sum_{j=0}^{n_a} q_i \cdot x(k-j) + d \cdot \sum_{j=0}^{n_v} p_i \cdot x(k-j) + c \cdot x(k) = u(k) - \sum_{j=0}^{n_x} r_j \cdot x(k-j) + \sum_{j=0}^{n_\delta} \Theta_j^T \cdot \delta(k-j) \quad (13)$$

This can be rewritten as an inverse model of the mechanical system:

$$u(k) = \sum_{j=0}^n g_j \cdot x(k-j) + \sum_{j=0}^{n_\delta} \Theta_j^T \cdot \delta(k-j) \quad (14)$$

with $n = \max \{n_a, n_v, n_x\}$ and $g_j = m \cdot q_j + d \cdot p_j + c + r_j$. This representation enables the possibility to model the inverse system dynamics with two FIR filters out of the displacement history. For further information see (Rizos *et al.* 2002a).

3. EXPERIMENTAL SET-UP

A one-dimensional guideway driven by a voice coil actuator produced by BEI-KIMCO was used for experimental analysis (see figure 4). The motor was driven by an analog amplifier, which provides the needed current with a high precision. The operating range of this system is 25 mm. Friction is introduced by the ball bearings of the guideway.

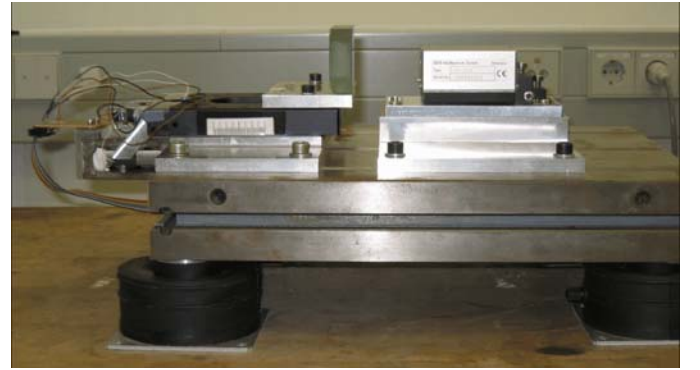


Fig. 4. Experimental set-up

The position is measured by a laser interferometer of the type SP-2000 (manufactured by SIOS Messtechnik GmbH) with a resolution below 0.1 nm (SIOS 2004). The test bed was assembled with parts of the Nanopositioning and Nanomeasuring Machine (Hausotte 2002). A modular dSpace® real-time hardware system in combination with Matlab/Simulink® was utilised for data acquisition and control. The position was sampled at a rate of 25 kHz and the control algorithm operated at a sampling rate of 6.25 kHz. More detailed information on the experimental set-up can be found in (Zimmermann *et al.* 2005). Since the motor force has a linear relationship with respect to the applied current, the motor force was calculated using the motor parameters provided by BEI-KIMCO.

3.1 Parameter Estimation Algorithm

The parameter identification algorithm proposed in (Rizos *et al.* 2002b) uses pairs of displacement-applied force signals to determine the model parameters via a quadratic cost function:

$$J = \sum_{k=\lambda}^N e^2(k) \quad (15)$$

$e^2(t)$ is calculated as the quadratic difference between the measured force $u(k)$, and the calculated force $\hat{u}(k)$:

$$e(k) = u(k) - \hat{u}(k) \quad (16)$$

Substituting Equ. (14) in Equ. (16) yields:

$$u(k) = \Phi^T \cdot [x(k) \dots x(k-n) ; \delta^T(k) \dots \delta^T(k-n_s) ; 1]^T + e(k) \quad (17)$$

$\Phi = [g_0 \dots g_n ; \Theta_0^T \dots \Theta_{n_s}^T ; b]$ contains all model parameters to be identified, including an additional offset. The model is linear with respect to Φ and nonlinear with respect to the threshold vector $d = [\Delta_1 \dots \Delta_M]$.

A sequential two-stage optimisation algorithm is used to identify the model parameters:

$$[d \ \Phi] = \arg \min_d \left\{ \min_{\Phi} J(\Phi, d) \right\} \quad (18)$$

In the first stage, a genetic algorithm is utilised to detect the areas of local minima in the parameter space (Houk *et al.* 1998). In the second stage the Nelder-Mead simplex algorithm is used to locate the global minimum in the regions provided in the first stage (Wernstedt 1989). In the case of the DNLRX model first the nonlinear threshold vector is identified followed by the linear model parameters. For initialisation of the proposed identification algorithm, initial values for the maximum deflection thresholds of the springs (Δ_i) are required. To find these initial values, a data pair is selected where the system is in the sliding regime. At this moment (t_{sl}) all Maxwell-Slip elements are sliding and the assumption $\delta_1 = \text{sgn}[x(t_{sl})] \cdot \Delta_1$ is satisfied.

To obtain an optimal identification result, the ‘dominant’ displacement extremum of the time series is selected. For the identification process only data pairs with $t > t_{sl}$ are used. To determine the quality of identification, the *normalised output error (NOE)* is utilized:

$$NOE = \left(\frac{\sum_{k=\lambda}^N (u(k) - \hat{u}(k))^2}{\sum_{k=\lambda}^N (u(k) - m_u)^2} \right) \times 100\% \quad (19)$$

Where m_u is the sample mean of the actual applied force, N the signal length (number of samples) and λ is specified in Equ. (15). While identifying the described system the model order was selected according to the algorithm proposed in Rizos *et al.* (2002a).

3.2 Identification Results

Figure 5 shows the identification data-set composed of the displacement (a) and the related applied force (b). The data-set consists of displacements in the sliding as well as in the pre-sliding regime. The data were low-pass filtered with a cutoff frequency of 50 Hz.

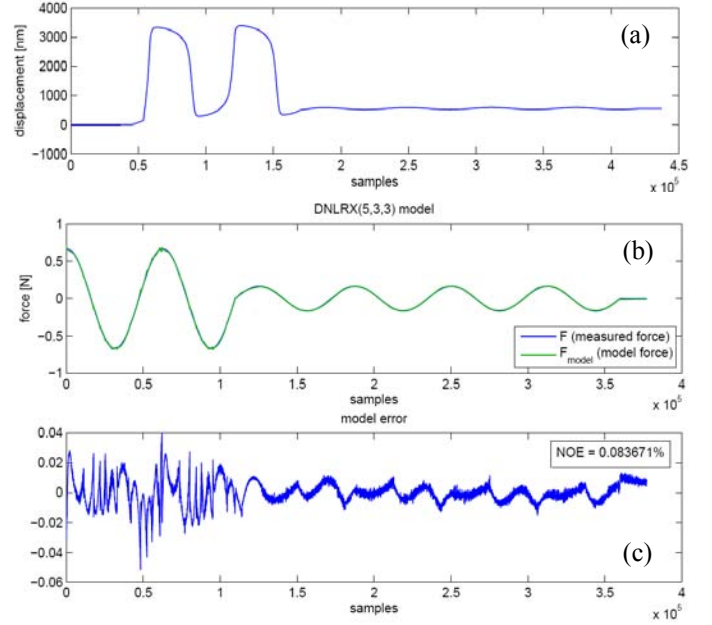


Fig. 5. Identification data-set: (a) displacement, (b) applied and predicted force, (c) model based error (NOE)

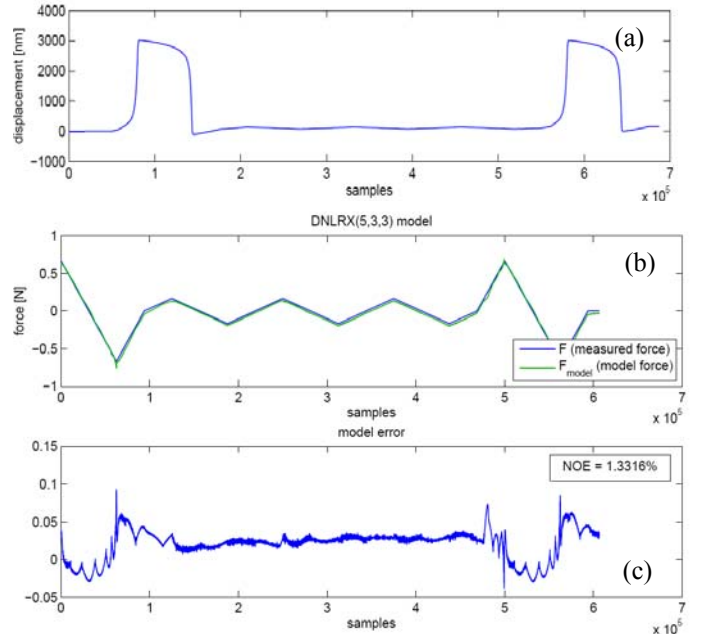


Fig. 6. Validation data-set: (a) displacement, (b) applied and predicted force, (c) model based error (NOE)

To speed up the identification process the algorithm was only carried out at every hundredth datapair. In comparison with an identification run using every data sample, the performance did not degrade significantly (about 0.01%) and the computing time was reduced by a factor of 30.

Regarding the model order, a DNLRX ($M=5, n_x=3, n_s=3$)

model leads to the best results. As shown in figure 3 (c), the NOE after identification is below 0.083%. This demonstrates the effectiveness of the proposed two-stage identification algorithm to find nearly a global minimum in the parameter space. Figure 6 shows the ability of the identified model to predict the system behaviour for a different validation dataset. In that case, the NOE is 1.33%. It should be mentioned that t_{sl} is the first sample of the plots in figure 5.

4. FRICTION COMPENSATION CONTROL

To verify the capability of the DNLRX model as part of a model-based control, we use this model in a feed-forward/feedback friction compensation scheme shown in figure 7. The advantage of such a control scheme is its potential to speed up the dynamic behaviour of a controlled system. It is thus possible for the controlled system to follow highly dynamic set points.

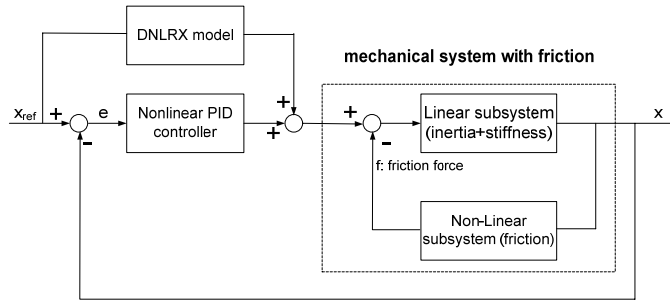


Fig. 7. Schematic diagram of the model-based friction compensation scheme proposed

With the friction compensation scheme the experimental set-up described in section 3 was controlled by a combination of a DNLRX based feed-forward controller and a nonlinear PID controller (Hausotte 2005) in the feedback loop.

While testing the feed-forward control with a DNLRX model of the order (5,3,3), a problem appeared. The DNLRX (5,3,3) sometimes predicted stepwise changes in the force $u(t)$. Figure 8 shows a zoomed version of figure 5(b).

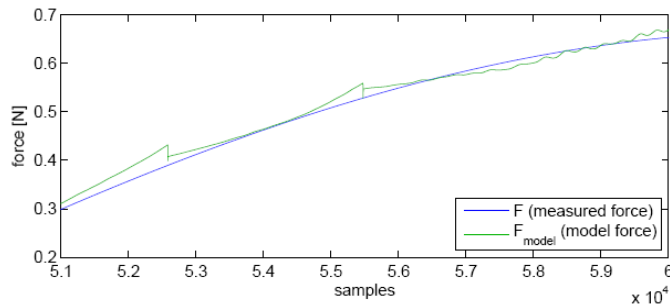


Fig. 8. Steps predicted by the DNLRX (5,3,3)

These steps cause large tracking errors on nanometer scale while using the DNLRX (5,3,3) as a feed-forward controller. Further examinations show that the steps were introduced by the second FIR filter from Equ. (14). In order to avoid this effect, we modified the model order to DNLRX (10,0,3). The identification effort and the identification quality are almost the same as before. The benefit of this modification is demonstrated in figure 9. With this adaptation it was possible

to predict the manipulated variable very precisely and smoothly.

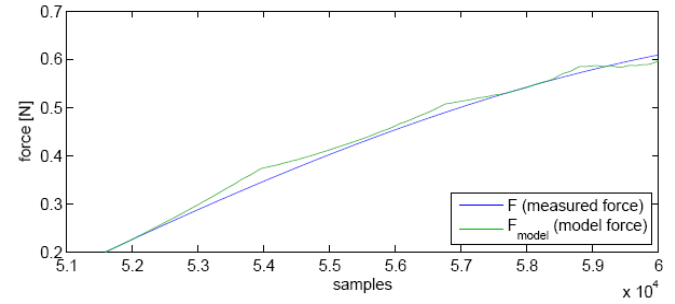


Fig. 9. Results of the DNLRX (10,0,3)

A sine trajectory with amplitude of 370 nm and a frequency of 1 Hz is applied as set-point to the control system. Figure 10 shows the behaviour of the controlled system without the DNLRX as a feed-forward controller. As it can easily be seen the PID controller is not able to follow the set-point trajectory.

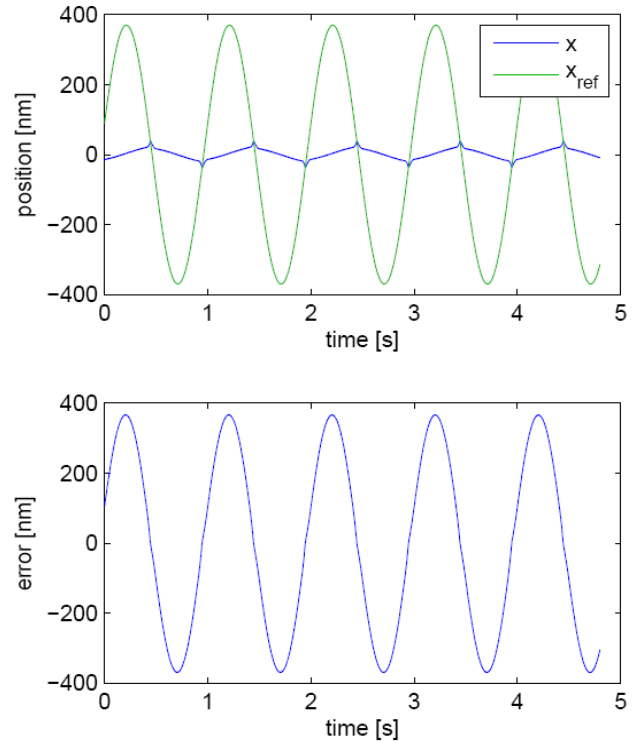


Fig. 10. Tracking performance without feed-forward control

If the DNLRX model is utilised as a feed-forward controller the hybrid control system is able to follow the trajectory (see figure 11) satisfactorily. Since the DNLRX model predicts the force which will be needed to reach the next set-point, the task of the feedback controller is only to compensate the model uncertainty and external disturbances. With the proposed model-based control design the tracking error can be reduced by a factor of nearly 100. Experiments also indicated that the DNLRX model is quite robust against disturbances, e.g. variations in temperature and so on.

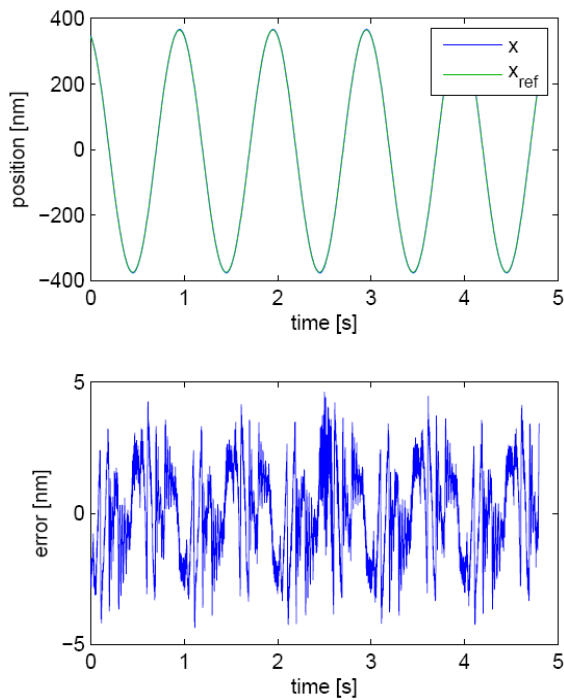


Fig. 11. Tracking performance with feedforward control

5. CONCLUSIONS

Modelling and control a mechanical system with friction on nanometer range is addressed. The identified model is used as a part of a highly dynamic controlling system, which is able to control the position on nanometer scale.

The DNLRX friction model is utilised to model the dynamics of a one-dimensional ball bearing guide on nanometer scale. The reason for selecting this model is its capability to capture nearly all nonlinear phenomena including the pre-sliding friction hysteresis with non-local memory. To obtain a proper model it is first necessary to implement the DNLRX model as well as a two-stage identification algorithm. After the implementation and identification process the usability of the DNLRX model to reflect the dynamic system behaviour is examined. The model is used as a feed-forward controller combined with a nonlinear PID controller in the feedback loop. After some modifications it can be shown that the DNLRX model is able to predict the system characteristics on the nanometer scale very precisely and reduce the tracking error by a factor of nearly 100.

Acknowledgements

The work was done within the framework of the Collaborative Research Centre 'Nanopositioning and Nanomeasuring Machines' at the Technische Universität of Ilmenau, which is supported by the German Research Foundation (DFG) and the Thuringian Ministry of Science. The authors would also like to thank all colleagues who offered help to the work presented.

References

Al-Bender, F., Fassois, S.D., Parltitz, U., Worden, K. (2007). Identification of Pre-Sliding and Sliding Friction Dynamics: Grey Box and Black Box Models. In:

- Mechanical Systems and Signal Processing*, Vol. 21, No. 1, pp. 514-534
- Armstrong-Héouvy, B., Dupont, P., De Wit, C. (1994). A survey of Models, Analysis Tools and Compensation Methods for Control of Machines with Friction. *Automatica*, Vol. 30, No. 7, pp. 1083-1138
- Dahl, P. (1968). A solid friction model. The Aerospace Corporation, El-Segundo, California, USA
- De Wit, C., Olsson, H., Aström, K.J., Lischinsky, P. (1995) A New Model for Control of Systems with Friction. In: *IEEE Transactions on Automatic Control*, Vol. 40 (3), pp. 419-425
- Dupont, P., Hayward, V., Armstrong, B., Alpeter, F. (2002). Single State Elasto-Plastic Friction Models, In: *IEEE Transactions on Automatic Control*, Vol. 47, No. 5, pp. 787-792
- Haessig, D., Friedland, B. (1991). On the Modeling and Simulation of Friction. In: *Proceedings of the 1990 American Control Conference*, Proceedings, pp. 1256-1261
- Houk, Ch. R., Joines, J. A., Kay, M. G. (1998). A Genetic Algorithm for Function Optimization: A Matlab Implementation. <http://www.ise.ncsu.edu/mirage/GAToolBox/gaot/>
- Hausotte, T. (2002). *Nanopositionier- und Nanomessmaschine*. Technische Universität Ilmenau, PhD Thesis, Ilmenau, Germany
- Hausotte, T. ; Jaeger, G. ; Manske, E. ; Sawodny, O. (2005). Control System of a Nanopositioning and Nanomeasuring Machine. In: *9th International Conference on New Actuators*. Proceedings, Bremen, Germany, pp. 123- 126
- Lampaert, V., Al-Bender, F., Swevers, J. (2002). Modification of the Leuven Integrated Friction Model Structure. In: *IEEE Transactions on Automatic Control*, Vol. 47, No. 4, pp. 683-687
- Lampaert, V., Al-Bender, F., Swevers, J. (2004). Experimental characterization of dry friction at low velocities on a developed tribometer setup for macroscopic measurements. In: *Tribology Letters*, Vol. 16, No. 1-2, pp. 95-105
- Lampaert, V., Al-Bender, F., Swevers, J. (2005). The Generalized Maxwell-Slip Model: A novel Model for Friction Simulation and Compensation. In: *IEEE Transactions on Automatic Control*, Vol. 50, No. 11, pp. 1883-1887
- Rizos, D.D., Fassois, S.D. (2005a). Maxwell Slip Model Based Identification and Control of Systems with Friction. In: *44th IEEE Conference on Decision and Control, and the European Control Conference 2005*, Proceedings, Sevilla, Spain, pp. 4578- 4583
- Rizos, D.D., Fassois, S.D. (2005b). Friction Identification based upon the LuGre and Maxwell Slip Models. In: *16th IFAC World Congress*, Proceedings, Prague
- SIOS Meßtechnik GmbH (2004). www.SIOS.de, Ilmenau, Germany
- Wernstedt, J. (1989). *Experimentelle Prozessanalyse*. Page 201-206, Verlag Technik, Berlin
- Zimmermann, J., Sawodny, O., Hausotte, T., Jaeger, G. (2005). Friction Modelling of a linear high-precision Actuator. In: *IFAC World Congress*, Proceedings, Prague